Interfacial Interactions and Segmental Dynamics of Poly(vinyl acetate)/Silica Nanocomposites

ARTICLE *in* THE JOURNAL OF PHYSICAL CHEMISTRY C · MAY 2015

Impact Factor: 4.77 · DOI: 10.1021/acs.jpcc.5b01240

6 AUTHORS, INCLUDING:

Yu Lin

East China University of Science and Technology

17 PUBLICATIONS **124** CITATIONS

SEE PROFILE

Gangmin Xu

Shanghai Normal University

1 PUBLICATION **0** CITATIONS

SEE PROFILE

THE JOURNAL OF PHYSICAL CHEMISTRY C

Article

pubs.acs.org/JPCC

Interfacial Interactions and Segmental Dynamics of Poly(vinyl acetate)/Silica Nanocomposites

Yu Lin, Langping Liu, Gangmin Xu, Dongge Zhang, Aiguo Guan, and Guozhang Wu*

Shanghai Key Laboratory of Advanced Polymeric Materials, School of Materials Science and Engineering, East China University of Science and Technology, Shanghai 200237, China

Supporting Information

ABSTRACT: We investigate the interfacial interactions and segmental dynamics of hydrophilic and hydrophobic (calcined) silica nanoparticle (NP) filled poly(vinyl acetate) (PVAc) composites via a combination of Fourier transform infrared spectroscopy (FTIR) and broadband dielectric spectroscopy measurements. For hydrophilic silica NP filled composites, an increase in the amount of bound carbonyl groups with increasing silica loading can be noted due to hydrogen bonding interactions with hydroxyls on the NP surfaces and carbonyl groups of PVAc. It is surprising that the apparent glass transition temperature (T_g) increases very slightly (~1 K) compared to pure PVAc, but the glass transition process becomes much broader, indicating the existence of a slower relaxation mode. In addition to the bulklike α-relaxation assigned to polymer segments away from the NP surfaces, the nanocomposites also exhibit a slower interfacial α'-relaxation by 3−4 orders of magnitude compared to bulk polymers. However, in the case of hydrophobic (calcined) silica NP filled composites, T_g shifts to higher temperatures by 4−5 K even if there is the absence of strong polymer-NP interfacial interactions confirmed by the FTIR results. Consequently, the overall α-relaxation dynamics are suppressed in the presence of silica NPs, which is attributed to an increase of steric hindrance and decrease of free volume. More importantly, in the nanocomposites with high NP loadings, it is worth noting a weak physical adsorption interfacial layer for which the segmental mobility is on average slower by 1−2 orders of magnitude relative to that for bulk polymers. However, the dielectric strength and interfacial bound fraction is much smaller than that of hydrophilic silica NP filled composites, indicating the fact that physical adsorption is much weaker compared to hydrogen bonding.

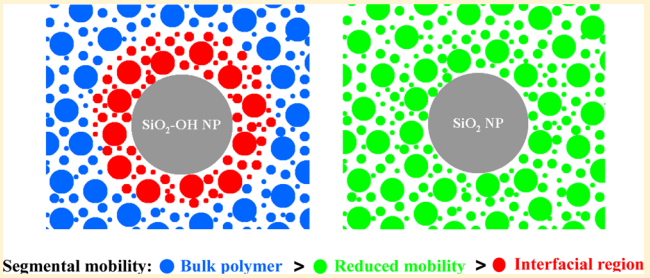

INTRODUCTION

It is generally accepted that the addition of nanoparticles (NPs) to polymer matrices can result in polymeric materials with significantly improved physicochemical properties such as mechanical strength or electrical conductivity.[1] A recurring challenge in the field of polymer nanocomposites (PNCs) is to quantitatively understand the polymer−NP interactions and mechanisms responsible for dynamics in a polymer matrix.[2,3] This issue is of critical importance since it is essential to direct the spatial distribution of NPs and thereby optimize a desired property of PNCs.[4,5] However, the main parameters that determine polymer−NP interactions and dynamics, and how they affect the macroscopic performance of such materials, are still inadequately understood to date and remain largely unresolved.

One of the most fundamental characteristics of amorphous polymers is the glass transition behavior which is directly related to the segmental mobility in polymeric materials. It is expected that the presence of interfaces due to the polymer−NP interactions may lead to changes in segmental mobility of the polymer especially for chains in the vicinity of NPs. In recent decades, numerous authors have investigated the effects of NP loading on the glass transition temperature (T_g) of PNCs with the aim of increasing the understanding of the dynamics of polymers close to interfaces.[6−11] However, experimental results of T_g shifts in PNCs are not conclusive concerning the complex characteristics of various polymers and NPs measured by different experimental techniques.[12−14] It has been reported that T_g increases compared to that of the bulk polymers due to immobilization of interfacial polymer chains.[9,15−17] On the other hand, incorporation of NPs leads to an acceleration of segmental mobility and T_g depression due to the increase of the free volume and decrease of the molecular packing density.[18−21] However, other studies demonstrated no change in the segmental dynamics related to T_g for PNCs.[8,10,22,23] In addition, two T_gs can be observed in the glass transition for some PNCs and the higher temperature relaxation peak corresponds to the interfacial close bounded chains.[24−27] These discrepancies are similar to contradictory results and interpretations of changes in the T_g of thin polymer films[17,28−30] or confined in nanopores.[31−33] Thus, the influence

Received: February 6, 2015
Revised: April 22, 2015
Published: May 19, 2015

DOI: 10.1021/acs.jpcc.5b01240
J. Phys. Chem. C 2015, 119, 12956−12966

of spatial confinement on the glass transition behaviors of polymers remains a great challenge.

Depending on the nature of the interactions (e.g., attractive or repulsive, hydrophilic or hydrophobic) at the polymer−NP or polymer−substrate interface, experiments have indicated that the relaxation dynamics of PNCs will either slow down or speed up.[16,17,34−37] Hence, by controlling the surface chemistry of NPs, the substrate of supported thin films, or the nanopore surface of polymers confined in nanopores, it should be possible to carefully tune the segmental dynamics of nanostructured materials. However, as previously reported, other investigations suggested that such controversies have little to do with strong interfacial or confinement effects,[2] but are more likely dependent on the thermal history and preparation method,[38] ambient atmosphere,[3] inadequate annealing treatment,[39−41] and measurement technique (spectroscopy, rheology, calorimetry, ellipsometry, etc.).[42] Therefore, a systematic study of the dynamics of the interfacial polymer and unraveling the role of the polymer−NP interaction is of great theoretical importance, and ultimately helpful for us to optimize the desired physicochemical properties of PNCs in various practical applications.

In the previous study, Schönhals et al.[43] investigated the interfacial interactions and dynamics of poly(vinyl acetate) (PVAc) adsorbed on silica particles, and found that relative strong hydrogen bonding can be formed between carbonyl groups of PVAc and hydroxyl groups on the surface of hydrophilic silica NPs. Herein, hydrophilic and hydrophobic (calcined) silica NP filled PVAc nanocomposites are chosen as model systems to investigate the interfacial interactions and quantitatively clarify their contributions to the segmental dynamics of interfacial bound layer and bulk polymer via a combination of Fourier transform infrared spectroscopy (FTIR) and broadband dielectric spectroscopy (BDS) measurements. Furthermore, we also emphasize recent controversies in studies of PNCs and polymer thin films by comparing results.

EXPERIMENTAL SECTION

Materials and Sample Preparation. Poly(vinyl acetate) (PVAc, $M_w = 6.9 \times 10^5$ g/mol, $M_w/M_n = 2.45$) was purchased from Sigma-Aldrich and used as received. Hydrophilic fumed silica NPs (VK-SP30, covered by hydroxyl groups, the number of hydroxyl groups is 2.9 per square nanometer of silica surface) with an average primary particle diameter of 30 nm and a BET surface area of 146 m^2/g, denoted as SiO_2−OH, were purchased from Hangzhou Wanjing New Material Co., Ltd., China. After hydrophilic silica NPs were treated by high temperature calcinations at 773 K for 6 h, the absorption band at 955 cm^{-1} assigned to vibrations of Si−OH groups cannot be seen from FTIR spectra (shown in Supporting Information, Figure S1), and the broad absorption band at 3450 cm^{-1} assigned to vibrations of hydroxyl groups was very weak, indicating the characteristic of hydrophobic silica NPs. These observations provided conclusive evidence that most of the hydroxyl groups on the surface of SiO_2−OH NPs were removed by calcination. Thus, hydrophobic silica NPs with the BET surface area of 138 m^2/g were obtained and denoted as SiO_2. It should be pointed out that a very small amount of hydroxyl groups at the hydrophobic (calcined) silica surface is very likely to exist, but the signal is too weak to be detected.

PVAc was dried at 333 K and various silica NPs were dried at 473 K in a vacuum oven for at least 8 h prior to use. The solution mixing method was employed to ensure a well-dispersed polymer nanocomposite. Different desired amounts of silica NPs were dispersed in chloroform and ultrasonicated for 30 min in a water bath. Then PVAc was added to the solution at a weight concentration of 5 wt % with continuous stirring for at least 48 h in order to ensure sufficient adsorption of PVAc chains on the surface of silica NPs. The solutions were then transferred to Teflon molds and placed at room temperature for 24 h. Finally, the samples were kept in a vacuum oven at 333 K for an additional 24 h to completely remove residual solvent, resulting in film thicknesses of approximately 100 μm. Thermogravimetric analysis (TGA) was performed to verify the NP weight fraction and the complete evaporation of solvent. Pure PVAc film was also obtained as bulk reference, and PVAc/silica nanocomposites at various NP concentrations (5, 15, and 30 wt %) were prepared using the above-mentioned method.

Characterization of the Nanocomposites. *Fourier Transform Infrared Spectroscopy (FTIR).* FTIR was applied to investigate the interfacial interactions between PVAc and silica NPs and obtain the quantitative information about the fraction of tightly bounded PVAc segments on the surface of silica NPs. Measurements were carried out at room temperature using a Nicolet 5700 FTIR spectroscope. The spectra were taken in transmittance mode in the wavenumber range from 400 to 4000 cm^{-1}, and a total of 32 scans were accumulated with the accuracy of 2 cm^{-1} for signal-averaging of each IR spectral measurement.

Broadband Dielectric Spectroscopy (BDS). BDS was employed to investigate the molecular mobility of interfacial and bulk PVAc segments in the PNCs. Dielectric measurements were performed on a Novocontrol Alpha high-resolution dielectric analyzer (Novocontrol GmbH Concept 40, Novocontrol Technology, Germany), and the temperature was controlled by a Novocool cryogenic system with a stability of ± 0.1 K. The films of 100 μm in thickness were placed between two parallel gold electrodes of 20 mm diameter. Isothermal frequency sweeps recording the dielectric function every 5 K were carried out over the temperature range from 293 to 393 K in the frequency range of 10^{-1}−10^7 Hz. Temperature sweeps were performed from 253 to 393 K at the frequency of 10 Hz and the heating rate of 3 K/min.

RESULTS AND DISCUSSION

Interfacial Interactions between PVAc and Silica NPs. It is expected that hydrophilic SiO_2−OH NPs experience attractive interactions with PVAc between the carbonyl groups of the polymer and hydroxyl groups on the silica surface. Figure 1 shows the FTIR spectra of pure PVAc and PVAc/SiO_2−OH nanocomposites with various NP loadings. Several characteristic absorption bands can be clearly extracted from the spectra.[43] Compared to the spectra of pure SiO_2−OH (shown in Supporting Information, Figure S1), a new pronounced absorption band located around 1738 cm^{-1} can be observed, which is assigned to the vibrations of the carbonyl groups in PVAc. Moreover, an absorption band at 1239 cm^{-1} for the C−O groups and a double peak around 1371 and 1436 cm^{-1} corresponding to vibrations of the CH_2 groups of PVAc can be identified from the spectra. The characteristic peaks observed in the pure SiO_2−OH (shown in Supporting Information, Figure S1), that is, the absorption bands around 1107 and 803 cm^{-1} for the vibrations of Si−O−Si and Si−O groups, respectively, become noticeable and increase with increasing silica loading. Similarly, the characteristic absorption bands of both PVAc and

DOI: 10.1021/acs.jpcc.5b01240
J. Phys. Chem. C 2015, 119, 12956−12966

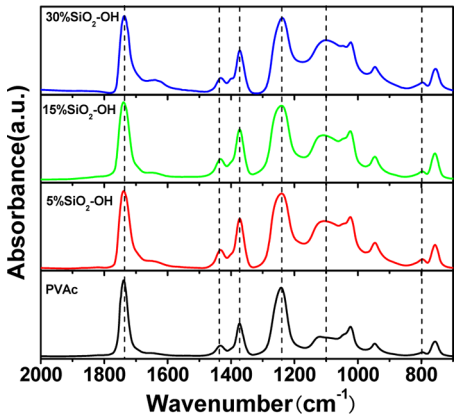

Figure 1. FTIR spectra of pure PVAc and PVAc/SiO_2−OH nanocomposites with various silica weight concentrations.

SiO_2 components can also be observed for PVAc/SiO_2 nanocomposites (shown in Supporting Information, Figure S2), and at the first glance there is no obvious difference between the spectra of hydrophilic and hydrophobic silica filled PVAc nanocomposites.

To quantitatively characterize the amount of interfacial bound PVAc chains, the spectra of the carbonyl region (1780−1640 cm^{-1}) is used to identify the vibrations of bound (hydrogen bonded) and free carbonyl groups in the nanocomposites. Figure 2 shows the normalized carbonyl band (with respect to the maximum value of the intensity of the absorption band of free carbonyl group at 1738 cm^{-1}) for different silica NP filled nanocomposites. Compared to the pure PVAc, it can be noted that the absorption band of carbonyl region broadens with increasing SiO_2−OH NP loading in the nanocomposites. Additionally, a pronounced shoulder peak develops located around 1705 cm^{-1}, which is assigned to stretching vibrations of hydrogen-bonded carbonyl groups to the NP surfaces.[43−46] However, the absorption band is almost independent of SiO_2 NP content and no obvious width broadening is observed for PVAc/SiO_2 nanocomposites, indicating that there is no hydrogen bonding interactions between the polymer and the hydrophobic silica NP surface.

As described in previous literature,[44−46] two Gaussians are used to obtain the satisfactory fitting of the absorption spectra after subtraction of the baseline, as shown in Figure 2c. The main absorption band at 1738 cm^{-1} due to free carbonyl groups originates from (i) the chains that are physically adsorbed on the NP surface but are not in interaction with the surface hydroxyl groups and (ii) the carbonyls of polymer chains far from the NPs, while the shoulder absorption peaks at low wavenumbers are attributed to the bound carbonyl groups resulting from the hydrogen bonding interactions with the NP surface. The integrated areas under the peaks correspond to the relative amount of free carbonyls (A_{free}) and bound carbonyl groups (A_{bound}), respectively. Accordingly, the fraction of interfacial bound carbonyl groups (X_{FTIR}) could be roughly calculated by taking the ratio of A_{bound} to the total area of carbonyl vibrations ($A_{total} = A_{free} + A_{bound}$). The values of X_{FTIR} versus silica concentration for PVAc/SiO_2−OH nanocomposites are listed in Table 1. With increasing SiO_2−OH NP loading, the fraction of bound carbonyl groups increases, indicating that the fraction of hydrogen-bonded segments increases. This occurs because the adsorption sites at the surface of SiO_2−OH NP increase with increasing silica content.

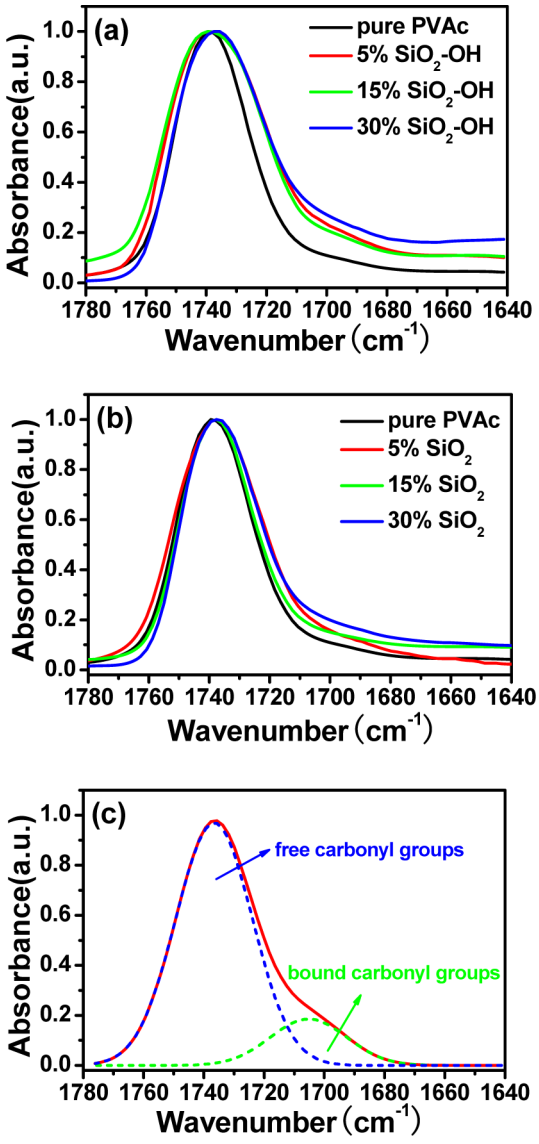

Figure 2. Normalized FTIR absorption spectra (carbonyl region) of (a) pure PVAc and PVAc/SiO_2−OH nanocomposites, and (b) PVAc/SiO_2 nanocomposites. (c) The dashed lines represent Gaussians fits to the data for the PVAc/SiO_2−OH 30% nanocomposite after subtraction of the baseline. The two peak areas correspond to free and bound carbonyl groups.

Table 1. Fraction of Bound Carbonyl Groups (A_{bound}/A_{total}) versus Hydrophilic Silica Concentration Obtained from FTIR Absorption Spectra of PVAc/SiO_2−OH Nanocomposites

silica weight concentration	$X_{FTIR} = A_{bound}/A_{total}$
5%	0.1122
15%	0.1417
30%	0.1607

However, a nonlinear relationship of bound fraction to the silica loading is presented, which might be attributed to the aggregate structure of NPs formed in the nanocomposites filled with high NP loadings. This is confirmed by the scanning electron microscopy (SEM) observations, as shown in Supporting Information, Figure S3. However, the dispersion of aggregates is reasonably homogeneous across the sample

DOI: 10.1021/acs.jpcc.5b01240
J. Phys. Chem. C 2015, 119, 12956−12966

area. Sangoro et al.[2] also found the aggregates of titania NPs in the poly(2-vinylpyridine) nanocomposites even at 3 vol % prepared by the solution mixing method.

Glass Transition Behaviors of PVAc/Silica Nanocomposites. As discussed above, the hydrogen bonding interactions between polymer chains and hydrophilic silica NP surfaces lead to the formation of a tightly "bound layer", while there is no interactions with the hydrophobic silica surface in PVAc/SiO_2 nanocomposites. Consequently, the glass transition behaviors of these two PNCs can be different, as shown in Supporting Information, Figure S4. The values of T_g can be determined from the peaks of tan δ curves. Figure 3a shows the changes of T_g versus silica NP loading for PVAc/silica nanocomposites. Compared to the bulk PVAc, only slight shifts of apparent T_g (~1 K) can be noted in hydrophilic silica NP filled PNCs even at loadings as high as 30 wt %. These results appear to be consistent with the invariant T_g observed in studies dealing with PVAc/silica nanocomposites[8,47] and other PNC systems.[10,22,23] These findings seem to contrast with the results of the increase of T_g[15−17] or appearance of another separate glass transition at higher temperature originating from restricted interfacial bound polymer chains in PNC systems with strong interfacial interactions.[24−27] On the one hand, it has been reported that the immobilized interfacial polymer is a so-called "dead layer", that is, completely immobilized with respect to the remaining polymer.[48−50] On the other hand, recent studies indicate that the interfacial dynamics are not immobilized via experimental analysis and theoretical simulations,[43,50−52] and then the glass transition of interfacial bound polymer chains can be observed. At first glance, one might conclude that the interfacial layer of PVAc/SiO_2−OH nanocomposites is immobilized related to the bulk polymers, and such a tightly bound layer with a few nanometers thickness does not undergo a glass transition as a whole. However, one can notice a clear asymmetric broadening of the glass transition behavior of the nanocomposites, as shown in Supporting Information, Figure S4a2. Such broaden effects can also be observed on the low-frequency sides of the isothermal dielectric loss curves with increasing SiO_2−OH NP concentration, as shown in Supporting Information, Figure S5a, indicating the existence of a slower dynamic process appearing on the low-frequency side of the segmental mode, which will be discussed in detail later. These results have been reported in previous literature for other NPs or additives-filled composites.[2,18,53] Hence, on the basis of the above discussion, this study provides conclusive evidence for the fact that the interfacial polymer layer is by no means a "dead layer".

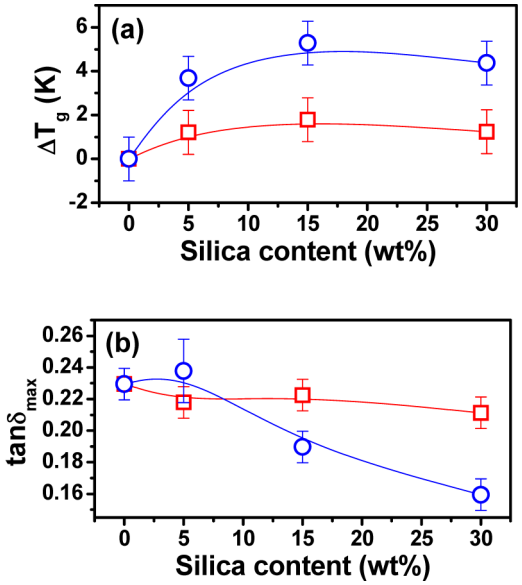

Figure 3. (a) T_g deviations and (b) tan δ peak values as a function of silica concentration for PVAc/SiO_2−OH nanocomposites (□) and PVAc/SiO_2 nanocomposites (○) detected by dielectric measurements.

In contrast, our results reveal that T_g increases by 4−5 K in PVAc nanocomposites with hydrophobic silica NP loadings of 5 to 30 wt %, as shown in Figure 3a. Such behaviors are in agreement with that of many other PNCs reported previously, in which the increased T_g and hindering polymer segmental mobility can be observed even in the absence of specific polymer-NP interactions.[15,16,54] This is also consistent with the findings in polymer thin and ultrathin films with decreasing thickness or annealing treatment.[17,39−41,55] As discussed above, there is no tightly interfacial bound layer in hydrophobic silica NP-filled PVAc nanocomposites due to the absence of strong polymer−NP interactions, and polymer chains can only undergo adsorption onto the NP surfaces via weak physical bond formation between the polymers and NP surfaces. As a result, hydrophobic silica NPs merely act as reinforcing fillers and participate in occupying the free volume of the polymer chains. Accordingly, the antiplasticization effects can be observed, that is, T_g increases and polymer segmental mobility decreases, due to an increase of the fragility of glass formation and the increased steric hindrance of polymer chains between NPs. However, no gradual increase of a broadening of the glass transition can be found in PVAc/SiO_2 nanocomposites, regardless of SiO_2 NP concentration, as shown in Supporting Information, Figure S4b2. This is borne out by the distribution width and symmetry of the isothermal dielectric spectra, as shown in Figure S5b, indicating the unchanged heterogeneous dynamics. A similar result has been reported in silica-filled PVAc composites by Roland et al.,[14] but differs from the ones confined in ultrathin polymer films.[40,56]

It is generally accepted that the peak intensity of dielectric loss tangent (tan δ) is dependent on the polymer chain mobility and proportional to the relative number of relaxing elements. Figure 3b shows the tan δ peak values as a function of silica loading for different PVAc/silica nanocomposites. The peak values of PVAc/SiO_2−OH nanocomposites are close to that of pure PVAc, and only a weak reduction tendency can be noted, which is consistent with the slight increase in T_g. This indicates that the segmental mobility is nearly unchanged by the introduction of SiO_2−OH NPs. However, it can be observed that the peak value decreases synchronously with increasing hydrophobic silica NP content in PVAc/SiO_2 nanocomposites, indicating the restricted mobility of polymer chains and reduced number of relaxing polymer segments. These results are interpreted as originating from a decrease in free volume and an increase in steric hindrance by the addition of SiO_2 NPs to PVAc matrix, which limits the mobility of polymer chains,[57] in agreement with the T_g results.

Segmental Dynamics of PVAc/Silica Nanocomposites. BDS is a powerful tool for studying the polymer dynamics and the polymer−NP interactions in NP-filled composites. This technique allows giving valuable information about both the segmental mobility of the polymer−NP interfacial and bulk polymer chains. Figure 4 shows the temperature and frequency

DOI: 10.1021/acs.jpcc.5b01240
J. Phys. Chem. C 2015, 119, 12956−12966

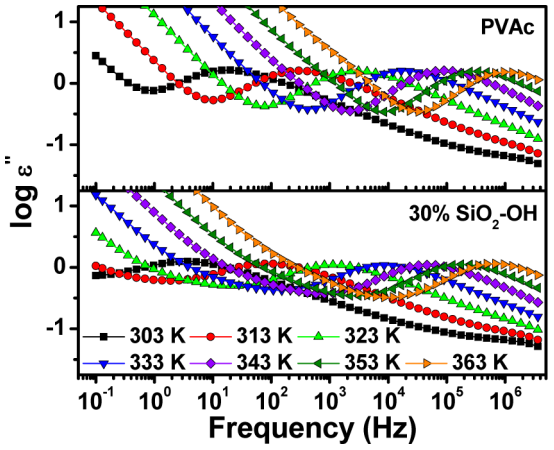

Figure 4. Dielectric loss as a function of frequency for pure PVAc and PVAc/SiO_2−OH-30% nanocomposite at various temperatures.

dependence of dielectric loss for pure PVAc and PVAc/SiO_2−OH-30% nanocomposite as representative examples. For pure PVAc, in addition to the ionic conductivity process at the low frequency side of the spectrum, only one relaxation peak identified as α-relaxation (dynamic glass transition) can be observed in the temperature range investigated, which is associated with the segmental motion of PVAc chains. However, the presence of SiO_2−OH NPs has a significant effect on the dielectric loss spectrum of PVAc, as shown in bottom spectra of Figure 4. The ionic conductivity contributions of PVAc/SiO_2−OH nanocomposites shift to lower frequencies compared to that of bulk PVAc at the same isothermal test temperature. Interestingly, a new pronounced second relaxation shoulder appears at lower frequencies relative to α-relaxation, which is assigned to the segmental relaxation of interfacial layer polymer chains whose mobility is restricted due to interactions with the NP surface. The dielectric relaxation processes of other PVAc/SiO_2−OH and PVAc/SiO_2 nanocomposites with various silica NP loadings will be discussed in detail later.

To extract quantitative information from the isothermal dielectric measurements, the empirical function of Havriliak−Negami (HN function) is used to analyze the complex dielectric data.[58]

$$\varepsilon^* = \varepsilon_\infty + \frac{\Delta\varepsilon}{[1 + (i\omega\tau_{HN})^{\alpha_{HN}}]^{\beta_{HN}}} - i\frac{\sigma}{\varepsilon_0\omega^s} \quad (1)$$

where ε_∞ is the unrelaxed value of the dielectric constant, $\Delta\varepsilon$ is the dielectric strength, ω is angular frequency ($\omega = 2\pi f$), τ_{HN} is the HN relaxation time, and the exponents α_{HN} and β_{HN} ($0 < \alpha_{HN}, \alpha_{HN}\beta_{HN} \leq 1$) are shape parameters that describe the symmetric and asymmetric broadening of the spectra, respectively. For the ionic conductivity contribution, σ is related to the specific dc conductivity, ε_0 is the dielectric permittivity of vacuum, and the coefficient s ($0 < s < 1$) characterizes the conduction mechanism. Furthermore, τ_{HN} is related to the mean molecular relaxation time τ_{max} corresponding to the maximum of the dielectric loss by the equation

$$\tau_{max} = \tau_{HN}\left(\sin\frac{\alpha_{HN}\beta_{HN}\pi}{2(\beta_{HN}+1)}\right)^{1/\alpha_{HN}}\left(\sin\frac{\alpha_{HN}\pi}{2(\beta_{HN}+1)}\right)^{-1/\alpha_{HN}} \quad (2)$$

Figure 5 shows the representative examples of fits of the HN function to the isothermal dielectric spectra of pure PVAc and

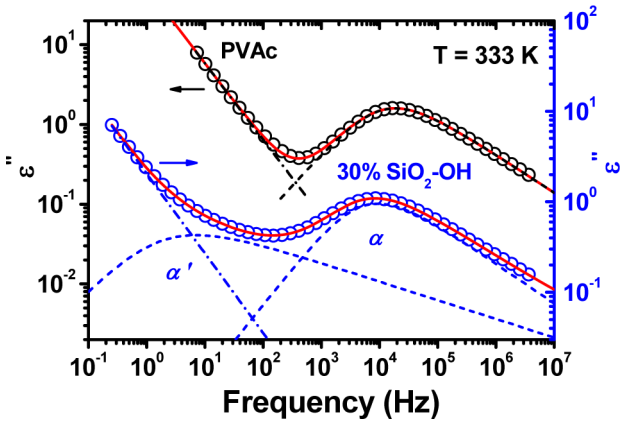

Figure 5. Dielectric loss as a function of frequency for pure PVAc and PVAc/SiO_2−OH-30% nanocomposite measured at 333 K. The solid lines are fits to the data using the HN function. The dashed dotted lines are the contribution of the conductivity. The dashed lines represent the segmental motion process, including bulklike segmental relaxation (α-relaxation) and interfacial segmental relaxation (α'-relaxation) processes.

PVAc/SiO_2−OH-30% nanocomposite at 333 K. A single HN function and conductivity process describes the data well for neat PVAc. However, such fit does not work for PVAc/SiO_2−OH nanocomposites because a single HN function is not sufficient to fit the dielectric loss data. Hence, two HN functions and a conductivity term are used to analyze the isothermal dielectric spectra. The high-frequency α-relaxation is associated with the segmental motion of PVAc chains which are far from the NP surfaces. The low-frequency α'-relaxation corresponds to the interfacial segmental relaxation of adsorbed PVAc chains on the NP surface. The shift to lower frequencies than that of bulklike polymer relaxation indicates that the molecular mobility of interfacial bound polymer is restricted due to hydrogen bonding interactions with the NP surface. Such suppressed dynamics of interfacial α'-relaxation has also been widely reported in other PNCs or geometric confined polymers with strong attractive interfacial interactions.[10,11,34,43,50,51,53,59,60]

The fits of HN functions to the isothermal dielectric spectra of PVAc/SiO_2−OH and PVAc/SiO_2 nanocomposites with different silica NP loadings can be found in Supporting Information, Figure S6. For hydrophilic SiO_2−OH NP filled PVAc composites, both bulklike α-relaxation and interfacial α'-relaxation can be observed for all the nanocomposites. Meanwhile, it is of note that the dielectric strength of α'-relaxation increases with increasing the concentration of SiO_2−OH NPs, indicating that the fraction of interfacial bound polymers increases, in good agreement with the FTIR results. However, only a weak interfacial α'-relaxation takes place in PVAc/SiO_2 nanocomposites with high SiO_2 NP loadings (30 wt %), while it is absent in PVAc/SiO_2-5% and 15% nanocomposites. As discussed above, polymer chains can only undergo adsorption onto the NP surfaces via weak physical adsorption due to the absence of hydrogen bonding interactions. Accordingly, the interfacial relaxation cannot be noted in the low concentration of SiO_2 NP-filled system because of the weak interfacial layer. Similarly, Giannelis et al.[61]

DOI: 10.1021/acs.jpcc.5b01240
J. Phys. Chem. C 2015, 119, 12956−12966

reported that the dielectric signal of interfacial mode is too weak to analyze quantitatively in carbon black-filled poly(styrene-*co*-butadiene) composites due to weak interfacial interactions. With increasing SiO_2 NP loading, a weak interfacial bound layer resulting from physical adsorption could be formed at very high NP concentrations (such as 30 wt %), and then the segmental relaxation of such a layer can be detected by sensitive dielectric measurements. Fragiadakis et al.[54] has also found the slower interfacial α'-relaxation of PNCs in the absence of specific polymer-filler interactions. However, the interfacial polymer relaxation strength of PVAc/SiO_2-30% nanocomposites is much weaker compared to hydrophilic SiO_2−OH NP filled composites, indicating much stronger interfacial interactions due to hydrogen bonding than physical adsorption.

Figure 6 shows the temperature dependences of τ_{max} of both bulklike α-relaxation and interfacial α'-relaxation for PVAc/SiO_2−OH and PVAc/SiO_2 nanocomposites, respectively, used to quantitatively analyze the impact of silica NP loading on the segmental relaxation times of PVAc composites. In the case of hydrophilic SiO_2−OH NP filled composites, it can be observed

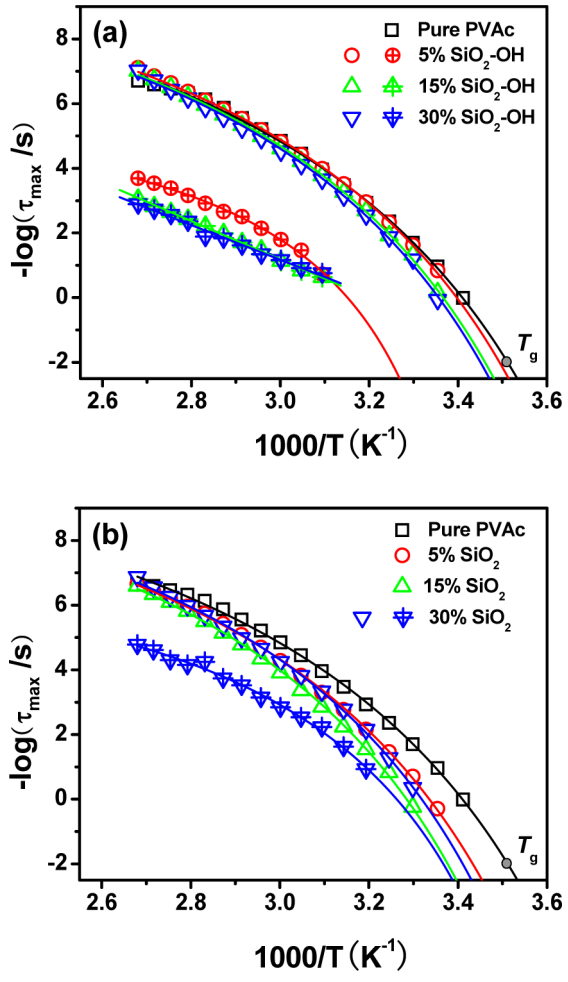

Figure 6. Bulklike segmental relaxation time (open symbols) and interfacial segmental dynamics (cross symbols) as a function of temperature for (a) PVAc/SiO_2−OH nanocomposites and (b) PVAc/SiO_2 nanocomposites. The solid curves represent VFT fits to the data. Arrhenius equations are used to fit the interfacial segmental relaxation processes of PVAc/SiO_2−OH nanocomposites with 15 and 30 wt % silica loadings.

that in addition to the bulklike polymer relaxation, the nanocomposites also exhibit slower relaxation times up to 3−4 orders of magnitude compared to bulk polymers, which is attributed to interfacial bound polymer relaxation. Such behaviors are expected for PNCs with strong attractive interfacial interactions and have been reported by many authors for the confined polymer systems in the literature[53,59,60] and predicted by molecular dynamics simulations.[51,52] These results can be interpreted as originating from the contributions of two distinct polymer chain motions: (i) The segmental dynamics of PVAc chains away from SiO_2−OH NPs are similar to the motions of the bulk chains because there is absence of interfacial interactions. Cangialosi et al.[47] and Roland et al.[8] also investigated that the local segmental dynamics of PVAc were unaffected by the presence of silica NPs. Similar results have been reported for other PNCs filled with silica NPs.[62−64] (ii) Because of hydrogen bonding interactions with the NP surface, the mobility of PVAc chains adjacent to SiO_2−OH NPs are strongly restricted, thus decreasing the interfacial segmental dynamics significantly. Nonetheless, no separate glass transition behavior is observed from the aforementioned T_g results.

However, the segmental relaxation dynamics are quite different for hydrophobic SiO_2 NP filled composites, as shown in Figure 6b. When the NP loading is lower than 15 wt %, α-relaxation time of the nanocomposites increases with an increase in the filler concentration, indicating the decreased polymer chain mobility due to an increase of steric hindrance and decrease of free volume. Such antiplasticization effects in PNCs have been reported in the literature by experimental observation[16,17,35,65,66] and predicted by simulations.[67,68] As the SiO_2 NP loading increases to 30 wt %, a weak physical adsorption interfacial layer could be formed at such a high NP content. Accordingly, apart from the decreased α-relaxation dynamics relative to pure PVAc which is assigned to polymer chains away from NP surfaces, the dielectric spectrum indicates an interfacial relaxation region where the segmental mobility is on average slower by 1−2 orders of magnitude compared to that of the bulk polymer. Fragiadakis et al.[54] and Holt et al.[50] also reported such slower interfacial segmental dynamics of NP-filled nanocomposites even in the absence of specific polymer−filler interactions. Besides, it should be noted that interfacial α'-relaxation times of PVAc/SiO_2-30% nanocomposites are faster by 1−2 orders of magnitude relative to that of PVAc/SiO_2−OH-30% nanocomposites, suggesting that physical adsorption is much weaker than hydrogen bonding interactions between the polymer and NP surfaces.

Furthermore, the temperature dependences of segmental relaxation time can be well described by the empirical Vogel−Fulcher−Tamman (VFT) equation

$$\tau_{max} = \tau_0 \exp\left(\frac{A}{T - T_0}\right) = \tau_0 \exp\left(\frac{DT_0}{T - T_0}\right) \quad (3)$$

where τ_0 is the infinite relaxation time and fixed to 10^{-12} s for the α-relaxation process to reduce fitting uncertainties,[69] A is related to the fragility of the system, D is the fragility strength parameter,[70] and T_0 is the Vogel temperature. Extrapolation of this fit to τ = 100 s gives the dielectric estimate of T_g (denoted as $T_{g,100s}$) from segmental relaxation. The solid lines in Figure 6 represent the VFT fits to the data. The parameters obtained from the fittings are listed in Table 2. For the bulklike α-relaxation of PVAc/SiO_2−OH nanocomposites, it is found that the estimated $T_{g,100s}$ is a little higher (2−5 K) than that of pure

DOI: 10.1021/acs.jpcc.5b01240
J. Phys. Chem. C 2015, 119, 12956−12966

Table 2. Relevant Fitting Parameters for the VFT Equation of PVAc/Silica Nanocomposites with Various Silica Concentrations

PVAc/silica nanocomposites	D	T_0 (K)	$T_{g,100s}$ (K)
pure PVAc	7.0	233.8	284.6
5% SiO_2−OH (α)	6.6	237.7	286.4
5% SiO_2−OH (α')[a]	2.1	277.4	307.9
15% SiO_2−OH	6.5	240.4	288.9
30% SiO_2−OH	6.5	241.1	289.7
5% SiO_2	6.8	240.3	291.0
15% SiO_2	6.5	246.4	296.1
30% SiO_2	6.4	244.4	292.9
30% SiO_2 (α')[a]	3.5	258.3	296.9

[a]The fitting values of τ_0 are $10^{-6.28}$ and $10^{-8.17}$ s for the interfacial segmental dynamics of PVAc/SiO_2−OH-5% nanocomposites and PVAc/SiO_2-30% nanocomposites, respectively.

PVAc, and the temperature dependences of τ_{max} of the bulklile polymer is essentially unaffected by the introduction of SiO_2−OH NPs. However, the interfacial bound layer of PVAc/SiO_2−OH-5% nanocomposite exhibits a relaxation time slower by approximately 3 orders of magnitude than that of neat PVAc, weaker temperature dependencies, and a much higher estimated $T_{g,100s}$ (23 K higher) from the VFT fit, indicating the restricted polymer chain mobility. In addition, it is interesting that the temperature dependences of α'-relaxation time of PVAc/SiO_2−OH-15% and 30% nanocomposites can be well described by an Arrhenius equation, $\tau = \tau_0 \exp(E_a/K_BT)$, where E_a is the mean activation energy and K_B is the Boltzmann's constant. This indicates the characteristic of strongly restricted interfacial relaxation. Barroso-Bujans et al.[34] also found such Arrhenius equation relations for the temperature dependences of α'-relaxation time of poly(ethylene oxide) confined in graphite oxide. The estimated values of E_a and τ_0 are 108 kJ/mol and 10^{-18} s for these two PVAc/SiO_2−OH nanocomposites, predicating the nearly identical α'-relaxation for both samples.

As for the hydrophobic SiO_2 NP filled composites, it can be observed that the α-relaxation time increases, and the estimated $T_{g,100s}$ shifts to higher temperatures (7−12 K higher), corresponding to the decrease of segmental mobility. In addition, the interfacial α'-relaxation time of the PVAc/SiO_2-30% nanocomposite is approximately 1−2 orders of magnitude slower than that of the bulk polymer, and exhibits a slightly weaker temperature dependence. The estimated $T_{g,100s}$ is 296.9 K from the VFT fit. Generally, T_g associated with the slower relaxation is used as a way to quantify the interfacial interaction strength between the polymer and the NP surface.[61] It can be noticed that the estimated interfacial relaxation T_g of PVAc/SiO_2−OH nanocomposites is much higher than that of SiO_2 filled composites, further indicating a stronger interfacial interaction (hydrogen bonding) in the composites containing SiO_2−OH NPs compared to physical adsorption in PVAc/SiO_2 nanocomposites.

Dielectric strength $\Delta\varepsilon$, which is proportional to the number density of dipoles involved in the relaxation process, reflects the molecular interaction to a particular degree. According to the Fröhlich−Kirkwood theory,[71,72] it is given by

$$\Delta\varepsilon = \frac{1}{3\varepsilon_0} g \frac{\mu^2}{K_B T} \frac{N}{V} \quad (4)$$

where g is the Kirkwood/Fröhlich correlation factor, μ is the dipole moment, and N/V is the number density of dipoles related to the process under consideration which is proportional to the concentration of PVAc chains involved in the relaxation process. Hence, similar to the FTIR results discussed above, the fraction of interfacial bound polymer (X_{BDS}) could be estimated from BDS measurements by taking the ratio of interfacial α'-relaxation dielectric strength $\Delta\varepsilon_{interface}$ to the total dielectric strength $\Delta\varepsilon_{total}$ ($\Delta\varepsilon_{total} = \Delta\varepsilon_{interface} + \Delta\varepsilon_{bulk}$), where $\Delta\varepsilon_{bulk}$ is the dielectric strength of bulklike α-relaxation. Figure 7a represents the temperature dependences of X_{BDS} for PVAc/SiO_2−OH nanocomposites. It is obvious that the bound fraction increases and is essentially independent of temperature with increasing SiO_2−OH NP loading, in good agreement with the FTIR data. This indicates that the interfacial bound polymer increases involved in the segmental relaxation process are due to an increase of hydrogen bonding adsorption sites at the NP surface with increasing silica NP content. However, it should be pointed out that the values of bound fractions estimated from the dielectric experiments are approximately 20% higher compared to the ones obtained from the carbonyl groups by FTIR analysis, which can be ascribed to different mechanisms, sensitivities, and measurement temperatures of these two techniques. It is worth mentioning that the dielectric measurement (tested at temperatures above T_g) is sensitive to molecular mobility, while a smaller volume is sensed via FTIR measurement (tested at room temperature) which is sensitive to bonding of groups.[43]

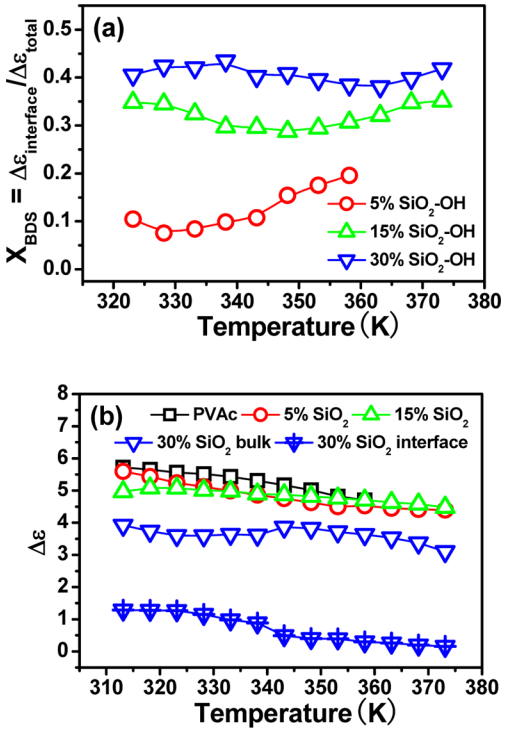

Figure 7. (a) Fraction of interfacial bound polymer defined as $\Delta\varepsilon_{interface}/\Delta\varepsilon_{total}$ versus temperature for PVAc/SiO_2−OH nanocomposites. (b) Temperature dependences of dielectric relaxation strengths of segmental relaxation processes for PVAc/SiO_2 nanocomposites. The cross symbol represents the dielectric relaxation strength of the interfacial segmental relaxation process for PVAc/SiO_2-30% nanocomposite.

DOI: 10.1021/acs.jpcc.5b01240
J. Phys. Chem. C 2015, 119, 12956−12966

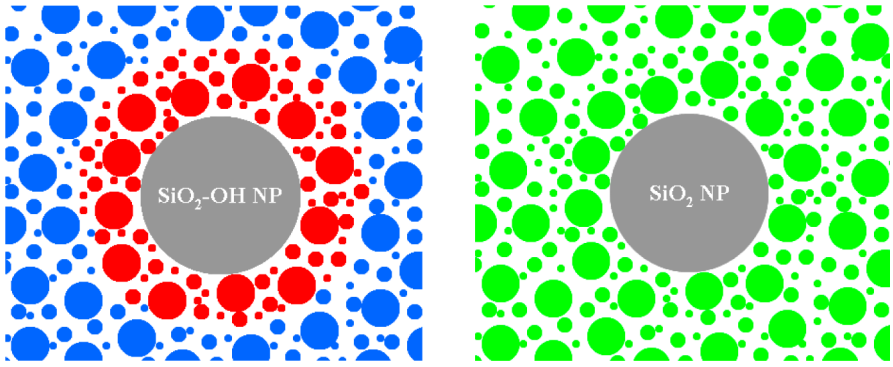

Figure 8. Schematic illustration of the segmental mobility of PVAc chains surrounding the silica surface in PVAc/silica nanocomposites. In PVAc/SiO_2−OH nanocomposites, the interfacial layer with strongly reduced mobility is due to interactions with hydroxyls on the NP surfaces and carbonyl groups of PVAc. The polymer segments away from the nanoparticles exhibit bulklike relaxation behavior, while only one segmental relaxation process with reduced mobility compared to bulk polymers can be observed in PVAc/SiO_2 nanocomposites. The order of segmental mobility is bulklike polymer (blue) > reduced mobility region (green) > interfacial region (red).

There is no interfacial segmental relaxation in PVAc/SiO_2 nanocomposites except for the 30 wt % SiO_2-filled sample because of the absence of strong polymer−NP interactions. Thus, the dielectric strengths $\Delta\varepsilon$ of different segmental relaxation processes are plotted versus temperature in Figure 7b for PVAc/SiO_2 nanocomposites. The $\Delta\varepsilon$ of α-relaxation decreases with increasing the filler content, indicating the reduced number of relaxing polymer segments and increase restriction of segmental mobility, which is consistent with the observed increase of T_g. In addition, a slight decrease of $\Delta\varepsilon$ can be observed with increasing temperature for the same nanocomposite, as indicated by the relationship between $\Delta\varepsilon$ and temperature shown in eq 4. For the PVAc/SiO_2-30% nanocomposite, the dielectric strength of interfacial α'-relaxation ($\Delta\varepsilon_{interface}$) is much smaller than that of bulklike α-relaxation ($\Delta\varepsilon_{bulk}$), suggesting a small bound fraction and weak interfacial layer merely due to physical adsorption. For the sake of illustrating the different effects of hydrogen bonding and physical adsorption on interfacial segmental relaxation, comparisons of X_{BDS} were made among hydrophilic and hydrophobic silica NP filled composites, as shown in Supporting Information, Figure S7. The interfacial bound fraction of PVAc/SiO_2 nanocomposites is much smaller compared to that of PVAc/SiO_2−OH nanocomposites with the same filler content, further confirming the fact that physical adsorption is much weaker than hydrogen bonding. These results are consistent with α'-relaxation dynamics showing a higher estimated interfacial relaxation $T_{g,100s}$ for SiO_2−OH NP filled composites.

Schematic Illustration of the Segmental Mobility in PVAc/Silica Nanocomposites. On the basis of the above discussions, we can draw the schematic illustration of the segmental mobility of PVAc chains in the silica NP filled nanocomposites, as shown in Figure 8. For PVAc/SiO_2−OH nanocomposites, the interfacial region with strongly reduced mobility is present due to interactions with hydroxyls on the NP surfaces and carbonyl groups of PVAc. Accordingly, such an interfacial bound layer exhibits segmental relaxation times slower by 3−4 orders of magnitude compared to bulk polymers. While the polymer segments away from the NPs exhibit bulklike relaxation behavior due to the absence of interfacial interactions. However, in the case of hydrophobic SiO_2 NP-filled PVAc composites, there is no hydrogen bonding interactions between the NP surfaces and polymer chains, thus only one segmental relaxation process with decreased mobility compared to pure PVAc can be observed in the nanocomposites due to the decrease of free volume and increase of steric hindrance by the introduction of presence of SiO_2 NPs. Moreover, in PVAc/SiO_2 nanocomposites filled with high NP contents, it is worth noting a weak physical adsorption interfacial layer whose segmental mobility is on average slower by 1−2 orders of magnitude compared to that of the bulk polymer. But the interfacial bound fraction X_{BDS} is much smaller than that of PVAc/SiO_2−OH nanocomposites, indicating that hydrogen bonding is much stronger relative to physical adsorption.

■ CONCLUSIONS

The interfacial interactions and segmental dynamics of hydrophilic and hydrophobic (calcined) silica NP-filled PVAc composites are characterized using a combination of FTIR and BDS measurements. The results reveal that the surface chemistry of silica NP has a pronounced effect on glass transition and segmental dynamics of the PNCs. For hydrophilic silica NP-filled composites, a pronounced shoulder peak of the FTIR spectra develops located around 1705 cm^{-1}, which is assigned to stretching vibrations of hydrogen-bonded carbonyl groups to the NP surfaces. The fraction of interfacial bound carbonyl groups X_{FTIR} increases with increasing silica NP loading. However, only a slight increase of T_g (~1 K) relative to pure PVAc can be noted for the PNCs even at the filler loading as high as 30 wt %, but a gradual asymmetric broadening of the glass transition can be found, indicating the existence of a slower dynamic process resulting from the restricted bound layer. The interfacial α'-relaxation exhibits segmental relaxation times slower by 3−4 orders of magnitude compared to bulk polymers. While the polymer segments away from the NP surfaces exhibit bulklike relaxation behavior. This indicates that the introduction of hydrophilic silica NPs simply slows down the segmental dynamics of the interfacial polymer region in the vicinity of NP surfaces. On the other hand, for hydrophobic (calcined) silica NP-filled composites, T_g shifts to higher temperatures by 4−5 K even in the absence of strong polymer−NP interfacial interactions, which is ascribed to an increase of steric hindrance and decrease of free volume by the introduction of silica NPs. Accordingly, we can notice an overall decreased α-relaxation dynamics and increased relaxation times. It is worth noting a weak physical adsorption

DOI: 10.1021/acs.jpcc.5b01240
J. Phys. Chem. C 2015, 119, 12956−12966

interfacial layer whose segmental mobility is on average slower by 1−2 orders of magnitude compared to that of the bulk polymer in the composites filled with high silica NP loadings. But the interfacial bound fraction X_{BDS} is much smaller, indicating that physical adsorption is much weaker compared to hydrogen bonding.

■ ASSOCIATED CONTENT

Supporting Information

FTIR spectra, SEM images, dielectric loss and interfacial bound fraction of silica NP-filled nanocomposites. The Supporting Information is available free of charge on the ACS Publications website at DOI: 10.1021/acs.jpcc.5b01240.

■ AUTHOR INFORMATION

Corresponding Author

*Tel.: +86-21-64251661. E-mail: wgz@ecust.edu.cn.

Notes

The authors declare no competing financial interest.

■ ACKNOWLEDGMENTS

This work was supported by the National Basic Research Program of China (2013CB035505), the National Nature Science Foundation of China (51373053), Shanghai Sailing Program (14YF1404900), China Postdoctoral Science Foundation (2015M571502), and the Fundamental Research Funds for the Central Universities.

■ REFERENCES

(1) Balazs, A. C.; Emrick, T.; Russell, T. P. Nanoparticle Polymer Composites: Where Two Small Worlds Meet. *Science* **2006**, *314*, 1107−1110.

(2) Holt, A. P.; Sangoro, J. R.; Wang, Y. Y.; Agapov, A. L.; Sokolov, A. P. Chain and Segmental Dynamics of Poly(2-vinylpyridine) Nanocomposites. *Macromolecules* **2013**, *46*, 4168−4173.

(3) Otegui, J.; Schwartz, G. A.; Cerveny, S.; Colmenero, J.; Loichen, J.; Westermann, S. Influence of Water and Filler Content on the Dielectric Response of Silica-Filled Rubber Compounds. *Macromolecules* **2013**, *46*, 2407−2416.

(4) Mackay, M. E.; Tuteja, A.; Duxbury, P. M.; Hawker, C. J.; Van Horn, B.; Guan, Z. B.; Chen, G. H.; Krishnan, R. S. General Strategies for Nanoparticle Dispersion. *Science* **2006**, *311*, 1740−1743.

(5) Kumar, S. K.; Jouault, N.; Benicewicz, B.; Neely, T. Nanocomposites with Polymer Grafted Nanoparticles. *Macromolecules* **2013**, *46*, 3199−3214.

(6) Arrighi, V.; McEwen, I. J.; Qian, H.; Prieto, M. B. S. The Glass Transition and Interfacial Layer in Styrene−Butadiene Rubber Containing Silica Nanofiller. *Polymer* **2003**, *44*, 6259−6266.

(7) Fragiadakis, D.; Pissis, P.; Bokobza, L. Glass Transition and Molecular Dynamics in Poly(dimethylsiloxane)/Silica Nanocomposites. *Polymer* **2005**, *46*, 6001−6008.

(8) Bogoslovov, R. B.; Roland, C. M.; Ellis, A. R.; Randall, A. M.; Robertson, C. G. Effect of Silica Nanoparticles on the Local Segmental Dynamics in Poly(vinyl acetate). *Macromolecules* **2008**, *41*, 1289−1296.

(9) Ding, Y. F.; Pawlus, S.; Sokolov, A. P.; Douglas, J. F.; Karim, A.; Soles, C. L. Dielectric Spectroscopy Investigation of Relaxation in C_{60}-Polyisoprene Nanocomposites. *Macromolecules* **2009**, *42*, 3201−3206.

(10) Hernandez, M.; Carretero-Gonzalez, J.; Verdejo, R.; Ezquerra, T. A.; Lopez-Manchado, M. A. Molecular Dynamics of Natural Rubber/Layered Silicate Nanocomposites as Studied by Dielectric Relaxation Spectroscopy. *Macromolecules* **2010**, *43*, 643−651.

(11) Raftopoulos, K. N.; Jancia, M.; Aravopoulou, D.; Hebda, E.; Pielichowski, K.; Pissis, P. POSS along the Hard Segments of Polyurethane. Phase Separation and Molecular Dynamics. *Macromolecules* **2013**, *46*, 7378−7386.

(12) Sargsyan, A.; Tonoyan, A.; Davtyan, S.; Schick, C. The Amount of Immobilized Polymer in PMMA SiO_2 Nanocomposites Determined from Calorimetric Data. *Eur. Polym. J.* **2007**, *43*, 3113−3127.

(13) Fragiadakis, D.; Pissis, P. Glass Transition and Segmental Dynamics in Poly(dimethylsiloxane)/Silica Nanocomposites Studied by Various Techniques. *J. Non-Cryst. Solids* **2007**, *353*, 4344−4352.

(14) Robertson, C. G.; Roland, C. M. Glass Transition and Interfacial Segmental Dynamics in Polymer−Particle Composites. *Rubber Chem. Technol.* **2008**, *81*, 506−522.

(15) Kropka, J. M.; Sakai, V. G.; Green, P. F. Local Polymer Dynamics in Polymer-C_{60} Mixtures. *Nano Lett.* **2008**, *8*, 1061−1065.

(16) Rittigstein, P.; Torkelson, J. M. Polymer−Nanoparticle Interfacial Interactions in Polymer Nanocomposites: Confinement Effects on Glass Transition Temperature and Suppression of Physical Aging. *J. Polym. Sci., Part B: Polym. Phys.* **2006**, *44*, 2935−2943.

(17) Rittigstein, P.; Priestley, R. D.; Broadbelt, L. J.; Torkelson, J. M. Model Polymer Nanocomposites Provide an Understanding of Confinement Effects in Real Nanocomposites. *Nat. Mater.* **2007**, *6*, 278−282.

(18) Hao, N.; Böhning, M.; Schönhals, A. Dielectric Properties of Nanocomposites Based on Polystyrene and Polyhedral Oligomeric Phenethyl-Silsesquioxanes. *Macromolecules* **2007**, *40*, 9672−9679.

(19) Hao, N.; Böhning, M.; Goering, H.; Schönhals, A. Nanocomposites of Polyhedral Oligomeric Phenethylsilsesquioxanes and Poly(bisphenol A carbonate) as Investigated by Dielectric Spectroscopy. *Macromolecules* **2007**, *40*, 2955−2964.

(20) Schönhals, A.; Goering, H.; Costa, F. R.; Wagenknecht, U.; Heinrich, G. Dielectric Properties of Nanocomposites Based on Polyethylene and Layered Double Hydroxide. *Macromolecules* **2009**, *42*, 4165−4174.

(21) Purohit, P. J.; Huacuja-Sánchez, J. E.; Wang, D. Y.; Emmerling, F.; Thünemann, A.; Heinrich, G.; Schönhals, A. Structure−Property Relationships of Nanocomposites Based on Polypropylene and Layered Double Hydroxides. *Macromolecules* **2011**, *44*, 4342−4354.

(22) Robertson, C. G.; Lin, C. J.; Rackaitis, M.; Roland, C. M. Influence of Particle Size and Polymer-Filler Coupling on Viscoelastic Glass Transition of Particle-Reinforced Polymers. *Macromolecules* **2008**, *41*, 2727−2731.

(23) Lin, Y.; Liu, L. P.; Cheng, J. Q.; Shangguan, Y. G.; Yu, W. W.; Qiu, B. W.; Zheng, Q. Segmental Dynamics and Physical Aging of Polystyrene/Silver Nanocomposites. *RSC Adv.* **2014**, *4*, 20086−20093.

(24) Tsagaropoulos, G.; Eisenberg, A. Dynamic Mechanical Study of the Factors Affecting the Two Glass Transition Behavior of Filled Polymers. Similarities and Differences with Random Ionomers. *Macromolecules* **1995**, *28*, 6067−6077.

(25) Tsagaropoulos, G.; Eisenburg, A. Direct Observation of Two Glass Transitions in Silica-Filled Polymers. Implications to the Morphology of Random Ionomers. *Macromolecules* **1995**, *28*, 396−398.

(26) Chen, L.; Zheng, K.; Tian, X. Y.; Hu, K.; Wang, R. X.; Liu, C.; Li, Y.; Cui, P. Double Glass Transitions and Interfacial Immobilized Layer in in-Situ-Synthesized Poly(vinyl alcohol)/Silica Nanocomposites. *Macromolecules* **2010**, *43*, 1076−1082.

(27) Robertson, C. G.; Rackaitis, M. Further Consideration of Viscoelastic Two Glass Transition Behavior of Nanoparticle-Filled Polymers. *Macromolecules* **2011**, *44*, 1177−1181.

(28) Alcoutlabi, M.; McKenna, G. B. Effects of Confinement on Material Behaviour at the Nanometre Size Scale. *J. Phys-Condens. Matter* **2005**, *17*, R461−R524.

(29) Mapesa, E. U.; Tress, M.; Schulz, G.; Huth, H.; Schick, C.; Reiche, M.; Kremer, F. Segmental and Chain Dynamics in Nanometric Layers of Poly(cis-1,4-Isoprene) as Studied by Broadband Dielectric Spectroscopy and Temperature-Modulated Calorimetry. *Soft Matter* **2013**, *9*, 10592−10598.

(30) Boucher, V. M.; Cangialosi, D.; Yin, H. J.; Schönhals, A.; Alegria, A.; Colmenero, J. T_g Depression and Invariant Segmental Dynamics in Polystyrene Thin Films. *Soft Matter* **2012**, *8*, 5119−5122.

DOI: 10.1021/acs.jpcc.5b01240
J. Phys. Chem. C 2015, 119, 12956−12966

(31) Li, L. L.; Zhou, D. S.; Huang, D. H.; Xue, G. Double Glass Transition Temperatures of Poly(methyl methacrylate) Confined in Alumina Nanotube Templates. *Macromolecules* **2014**, *47*, 297−303.
(32) Suzuki, Y.; Duran, H.; Steinhart, M.; Butt, H. J.; Floudas, G. Homogeneous Crystallization and Local Dynamics of Poly(ethylene oxide) (PEO) Confined to Nanoporous Alumina. *Soft Matter* **2013**, *9*, 2621−2628.
(33) Blaszczyk-Lezak, I.; Hernandez, M.; Mijangos, C. One Dimensional PMMA Nanofibers from AAO Templates. Evidence of Confinement Effects by Dielectric and Raman Analysis. *Macromolecules* **2013**, *46*, 4995−5002.
(34) Barroso-Bujans, F.; Cerveny, S.; Alegria, A.; Colmenero, J. Chain Length Effects on the Dynamics of Poly(ethylene oxide) Confined in Graphite Oxide: A Broadband Dielectric Spectroscopy Study. *Macromolecules* **2013**, *46*, 7932−7939.
(35) Bansal, A.; Yang, H. C.; Li, C. Z.; Cho, K. W.; Benicewicz, B. C.; Kumar, S. K.; Schadler, L. S. Quantitative Equivalence between Polymer Nanocomposites and Thin Polymer Films. *Nat. Mater.* **2005**, *4*, 693−698.
(36) Moll, J.; Kumar, S. K. Glass Transitions in Highly Attractive Highly Filled Polymer Nanocomposites. *Macromolecules* **2012**, *45*, 1131−1135.
(37) Zheng, F. F.; Zuo, B.; Zhu, Y. M.; Yang, J. P.; Wang, X. P. Probing Substrate Effects on Relaxation Dynamics of Ultrathin Poly(vinyl acetate) Films by Dynamic Wetting of Water Droplets on Their Surfaces. *Soft Matter* **2013**, *9*, 11680−11689.
(38) Tress, M.; Erber, M.; Mapesa, E. U.; Huth, H.; Muller, J.; Serghei, A.; Schick, C.; Eichhorn, K. J.; Volt, B.; Kremer, F. Glassy Dynamics and Glass Transition in Nanometric Thin Layers of Polystyrene. *Macromolecules* **2010**, *43*, 9937−9944.
(39) Lin, Y.; Tan, Y. Q.; Qiu, B. W.; Shangguan, Y. G.; Harkin-Jones, E.; Zheng, Q. Influence of Annealing on Chain Entanglement and Molecular Dynamics in Weak Dynamic Asymmetry Polymer Blends. *J. Phys. Chem. B* **2013**, *117*, 697−705.
(40) Nguyen, H. K.; Labardi, M.; Capaccioli, S.; Lucchesi, M.; Rolla, P.; Prevosto, D. Interfacial and Annealing Effects on Primary Alpha-Relaxation of Ultrathin Polymer Films Investigated at Nanoscale. *Macromolecules* **2012**, *45*, 2138−2144.
(41) Nguyen, H. K.; Labardi, M.; Lucchesi, M.; Rolla, P.; Prevosto, D. Plasticization in Ultrathin Polymer Films: The Role of Supporting Substrate and Annealing. *Macromolecules* **2013**, *46*, 555−561.
(42) Boucher, V. M.; Cangialosi, D.; Alegria, A.; Colmenero, J.; Pastoriza-Santos, I.; Liz-Marzan, L. M. Physical Aging of Polystyrene/Gold Nanocomposites and Its Relation to the Calorimetric T_g Depression. *Soft Matter* **2011**, *7*, 3607−3620.
(43) Fullbrandt, M.; Purohit, P. J.; Schönhals, A. Combined FTIR and Dielectric Investigation of Poly(vinyl acetate) Adsorbed on Silica Particles. *Macromolecules* **2013**, *46*, 4626−4632.
(44) Berquier, J.-M.; Arribart, H. Attenuated Total Reflection Fourier Transform Infrared Spectroscopy Study of Poly(methyl methacrylate) Adsorption on a Silica Thin Film: Polymer/Surface Interactions. *Langmuir* **1998**, *14*, 3716−3719.
(45) Krisanangkura, P.; Packard, A. M.; Burgher, J.; Blum, F. D. Bound Fractions of Methacrylate Polymers Adsorbed on Silica Using FTIR. *J. Polym. Sci., Part B: Polym. Phys.* **2010**, *48*, 1911−1918.
(46) Maddumaarachchi, M.; Blum, F. D. Thermal Analysis and FT-IR Studies of Adsorbed Poly(ethylene-stat-vinyl acetate) on Silica. *J. Polym. Sci., Part B: Polym. Phys.* **2014**, *52*, 727−736.
(47) Boucher, V. M.; Cangialosi, D.; Alegria, A.; Colmenero, J. Time Dependence of the Segmental Relaxation Time of Poly(vinyl acetate)-Silica Nanocomposites. *Phys. Rev. E* **2012**, *86*, 041501.
(48) Napolitano, S.; Wubbenhorst, M. Dielectric Signature of a Dead Layer in Ultrathin Films of a Nonpolar Polymer. *J. Phys. Chem. B* **2007**, *111*, 9197−9199.
(49) Rotella, C.; Wubbenhorst, M.; Napolitano, S. Probing Interfacial Mobility Profiles via the Impact of Nanoscopic Confinement on the Strength of the Dynamic Glass Transition. *Soft Matter* **2011**, *7*, 5260−5266.
(50) Holt, A. P.; Griffin, P. J.; Bocharova, V.; Agapov, A. L.; Imel, A. E.; Dadmun, M. D.; Sangoro, J. R.; Sokolov, A. P. Dynamics at the Polymer/Nanoparticle Interface in Poly(2-vinylpyridine)/Silica Nanocomposites. *Macromolecules* **2014**, *47*, 1837−1843.
(51) Ghanbari, A.; Rahimi, M.; Dehghany, J. Influence of Surface Grafted Polymers on the Polymer Dynamics in a Silica−Polystyrene Nanocomposite: A Coarse-Grained Molecular Dynamics Investigation. *J. Phys. Chem. C* **2013**, *117*, 25069−25076.
(52) Gao, Y. Y.; Liu, J.; Zhang, L. Q.; Cao, D. P. Existence of a Glassy Layer in the Polymer-Nanosheet Interface: Evidence from Molecular Dynamics. *Macromol. Theor. Simul.* **2014**, *23*, 36−48.
(53) Hernandez, M.; Ezquerra, T. A.; Verdejo, R.; Lopez-Manchado, M. A. Role of Vulcanizing Additives on the Segmental Dynamics of Natural Rubber. *Macromolecules* **2012**, *45*, 1070−1075.
(54) Fragiadakis, D.; Bokobza, L.; Pissis, P. Dynamics near the Filler Surface in Natural Rubber−Silica Nanocomposites. *Polymer* **2011**, *52*, 3175−3182.
(55) Napolitano, S.; Wubbenhorst, M. The Lifetime of the Deviations from Bulk Behaviour in Polymers Confined at the Nanoscale. *Nat. Commun.* **2011**, *2*, 260.
(56) Nguyen, H. K.; Prevosto, D.; Labardi, M.; Capaccioli, S.; Lucchesi, M.; Rolla, P. Effect of Confinement on Structural Relaxation in Ultrathin Polymer Films Investigated by Local Dielectric Spectroscopy. *Macromolecules* **2011**, *44*, 6588−6593.
(57) Yu, W. W.; Du, M.; Ye, W. J.; Lv, W. Y.; Zheng, Q. Relaxation Behavior of Layered Double Hydroxides Filled Dangling Chain-Based Polyurethane/Polymethyl Methacrylate Nanocomposites. *Polymer* **2014**, *55*, 2455−2463.
(58) Havriliak, S.; Negami, S. A Complex Plane Representation of Dielectric and Mechanical Relaxation Processes in Some Polymers. *Polymer* **1967**, *8*, 161−210.
(59) Klonos, P.; Panagopoulou, A.; Bokobza, L.; Kyritsis, A.; Peoglos, V.; Pissis, P. Comparative Studies on Effects of Silica and Titania Nanoparticles on Crystallization and Complex Segmental Dynamics in Poly(dimethylsiloxane). *Polymer* **2010**, *51*, 5490−5499.
(60) Hernandez, M.; Bernal, M. D.; Verdejo, R.; Ezquerra, T. A.; Lopez-Manchado, M. A. Overall Performance of Natural Rubber/Graphene Nanocomposites. *Compos. Sci. Technol.* **2012**, *73*, 40−46.
(61) Vo, L. T.; Anastasiadis, S. H.; Giannelis, E. P. Dielectric Study of Poly(styrene-co-butadiene) Composites with Carbon Black, Silica, and Nanoclay. *Macromolecules* **2011**, *44*, 6162−6171.
(62) Boucher, V. M.; Cangialosi, D.; Alegria, A.; Colmenero, J.; Gonzalez-Irun, J.; Liz-Marzan, L. M. Accelerated Physical Aging in PMMA/Silica Nanocomposites. *Soft Matter* **2010**, *6*, 3306−3317.
(63) Cangialosi, D.; Boucher, V. M.; Alegria, A.; Colmenero, J. Enhanced Physical Aging of Polymer Nanocomposites: The Key Role of the Area to Volume Ratio. *Polymer* **2012**, *53*, 1362−1372.
(64) Schneider, G. J.; Nusser, K.; Willner, L.; Falus, P.; Richter, D. Dynamics of Entangled Chains in Polymer Nanocomposites. *Macromolecules* **2011**, *44*, 5857−5860.
(65) Moll, J. F.; Akcora, P.; Rungta, A.; Gong, S. S.; Colby, R. H.; Benicewicz, B. C.; Kumar, S. K. Mechanical Reinforcement in Polymer Melts Filled with Polymer Grafted Nanoparticles. *Macromolecules* **2011**, *44*, 7473−7477.
(66) Harton, S. E.; Kumar, S. K.; Yang, H. C.; Koga, T.; Hicks, K.; Lee, E.; Mijovic, J.; Liu, M.; Vallery, R. S.; Gidley, D. W. Immobilized Polymer Layers on Spherical Nanoparticles. *Macromolecules* **2010**, *43*, 3415−3421.
(67) Betancourt, B. A. P.; Douglas, J. F.; Starr, F. W. Fragility and Cooperative Motion in a Glass-Forming Polymer−Nanoparticle Composite. *Soft Matter* **2013**, *9*, 241−254.
(68) Starr, F. W.; Douglas, J. F. Modifying Fragility and Collective Motion in Polymer Melts with Nanoparticles. *Phys. Rev. Lett.* **2011**, *106*, 115702.
(69) Kremer, F.; Schönhals, A. *Broadband Dielectric Spectroscopy*; Springer: Berlin, 2003.
(70) Richert, R.; Angell, C. A. Dynamics of Glass-Forming Liquids. V. On the Link between Molecular Dynamics and Configurational Entropy. *J. Chem. Phys.* **1998**, *108*, 9016−9026.

DOI: 10.1021/acs.jpcc.5b01240
J. Phys. Chem. C 2015, 119, 12956−12966

(71) Kirkwood, J. G. The Dielectric Polarization of Polar Liquids. *J. Chem. Phys.* **1939**, *7*, 911−919.
(72) Frölich, H. *Theory of Dielectrics: Dielectric Constant and Dielectric Loss*; Clarendon Press: Oxford, 1949.

DOI: 10.1021/acs.jpcc.5b01240
J. Phys. Chem. C 2015, 119, 12956−12966